Field-induced effects of anisotropic magnetic interactions in $SrCu_2(BO_3)_2$

2005 J. Phys.: Condens. Matter 17 L61

(http://iopscience.iop.org/0953-8984/17/4/L02)

INSTITUTE OF PHYSICS PUBLISHING JOURNAL OF PHYSICS: CONDENSED MATTER

J. Phys.: Condens. Matter **17** (2005) L61–L68 doi:10.1088/0953-8984/17/4/L02

LETTER TO THE EDITOR

Field-induced effects of anisotropic magnetic interactions in $SrCu_2(BO_3)_2$

K Kodama[1], S Miyahara[2], M Takigawa[1,7], M Horvatić[3], C Berthier[3,4], F Mila[5], H Kageyama[6] and Y Ueda[1]

[1] Institute for Solid State Physics, University of Tokyo, Kashiwanoha, Kashiwa, Chiba 277-8581, Japan
[2] Department of Physics, Aoyama Gakuin University, Sagamihara, Kanagawa 229-8558, Japan
[3] Grenoble High Magnetic Field Laboratory, CNRS and MPI-FKF, BP 166-38042 Grenoble, France
[4] Laboratoire de Spectrométrie Physique, Université J Fourier, BP 87-38402 St.Martin d'Hères, France
[5] Institute of Theoretical Physics, Ecole Polytechnique Fédérale de Lausanne, CH-1015 Lausanne, Switzerland
[6] Department of Chemistry, Graduate School of Science, Kyoto University, Kyoto 606-8502, Japan

E-mail: masashi@issp.u-tokyo.ac.jp

Received 22 November 2004, in final form 4 January 2005
Published 14 January 2005
Online at stacks.iop.org/JPhysCM/17/L61

Abstract

We observed a field-induced staggered magnetization in the 2D frustrated dimer singlet spin system $SrCu_2(BO_3)_2$ by ^{11}B NMR, from which the magnitudes of the intradimer Dzyaloshinsky–Moriya interaction and the staggered g-tensor were determined. These anisotropic interactions cause singlet–triplet mixing and eliminate a quantum phase transition at the expected critical field H_c for gap closing. They provide a quantitative account for some puzzling phenomena such as the onset of a uniform magnetization below H_c and the persistence of the excitation gap above H_c. The gap was accurately determined from the activation energy of the nuclear relaxation rate.

Spin systems with singlet ground states exhibit a variety of quantum phase transitions in magnetic field [1]. A generic example is the Bose–Einstein condensation of triplets when the field exceeds the critical value at which the excitation energy vanishes. This results in an antiferromagnetic order with the staggered moment perpendicular to the field, as has been observed, e.g., in $TlCuCl_3$ [2]. Another possibility is the formation of a superlattice of localized triplets due to repulsive interactions, which translates into magnetization plateaus at fractional values of the saturated magnetization. The best known example is $SrCu_2(BO_3)_2$ with its

[7] Author to whom any correspondence should be addressed.

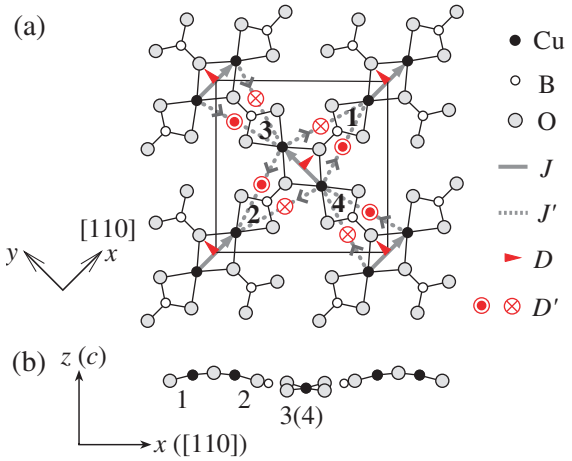

Figure 1. The magnetic layer of $SrCu_2(BO_3)_2$ viewed along (a) the c-(z-) and (b) the $[1\bar{1}0]$-(y-) directions. Numbers are the site indices for both Cu and B. Symbols for D and D' indicate the direction of $\boldsymbol{d}$ in the Dzyaloshinsky–Moriya interaction $\boldsymbol{d}\cdot(\boldsymbol{s}_i \times \boldsymbol{s}_j)$ with the bond direction $i \to j$ shown by arrows.

(This figure is in colour only in the electronic version)

two-dimensional network of orthogonal dimers of Cu^{2+} ions (spin 1/2). This material shows an excitation gap $\Delta_0 = 35$ K and plateaus at one-eighth, one-quarter, and one-third of the saturated magnetization [3–5]. A magnetic superlattice at the 1/8-plateau has actually been observed by NMR experiments [6].

These basic properties can be explained by a Heisenberg model on the frustrated Shastry–Sutherland lattice,

$$\mathcal{H}_0 = J \sum_{nn} \boldsymbol{s}_i \cdot \boldsymbol{s}_j + J' \sum_{nnn} \boldsymbol{s}_i \cdot \boldsymbol{s}_j, \tag{1}$$

where J and J' are the intra- and interdimer exchange interactions as shown in figure 1(a) [3, 7]. However, several aspects of low-temperature and high-field properties remain mysterious:

(i) a finite magnetization appears well below the expected critical field for the gap closing $H_c = \Delta_0/g_z\mu_B$, where g_z is the g-value along the field direction [5, 8];
(ii) a gap seems to persist above H_c [9–11];
(iii) there appears no phase transition down to $T = 0$ at fields below the 1/8-plateau, which means that no Bose condensation occurs, while one has been observed above it [11];
(iv) the magnetization shows a discontinuous jump at the lower boundary of the 1/8-plateau [6, 8].

Properties (i) and (ii) suggest that triplet states are mixed into the ground state by some anisotropic interactions. The *interdimer* Dzyaloshinsky–Moriya (DM) interaction,

$$\mathcal{H}' = \sum_{nnn} D'_{ij}(s_i^x s_j^y - s_i^y s_j^x), \tag{2}$$

where $|D'_{ij}| = D'$ and the sign alternates as shown in figure 1(a), was required to explain the splitting of triplet energy levels [12, 9]. However, it does not have matrix elements between singlet and one-triplet states. Although the *intradimer* DM interaction is a candidate, no estimate for its magnitude has been made so far.

In this letter, we report observation of a field-induced staggered magnetization by ^{11}B NMR experiments, which is also caused by singlet–triplet mixing. Quantitative estimates of the intradimer DM interaction and the staggered g-tensor are obtained. Furthermore, these anisotropic interactions provide quantitative accounts for the above points (i) and (ii). We also report the behaviour of the gap obtained from the nuclear relaxation rate upon entering into the 1/8-plateau.

A single crystal of $SrCu_2(BO_3)_2$ was grown by the travelling-solvent-floating-zone method using $LiBO_2$ solvent [13]. The NMR measurements below 18 T were performed at ISSP, University of Tokyo, while data at higher fields were obtained using a 20 MW resistive magnet at the Grenoble High-Magnetic-Field Laboratory.

We first describe the anisotropic interactions compatible with the crystal structure (space group $I\bar{4}2m$ [14]). A crucial feature is the non-coplanar buckling of the magnetic $CuBO_3$ layers as depicted in figure 1(b). This allows additional anisotropic interactions,

$$\mathcal{H}_1 = -\mu_B \boldsymbol{H} \cdot \left(\sum_{i=1}^{4} \mathbf{g}_i \cdot \boldsymbol{s}_i \right) + D \left\{ \sum_{A} (s_1^z s_2^x - s_1^x s_2^z) - \sum_{B} (s_3^y s_4^z - s_3^z s_4^y) \right\}, \tag{3}$$

where A (B) denotes dimers along the x- ($y-$) direction. The second term, the intradimer DM interaction, is allowed since the buckling breaks inversion symmetry at the centre of the dimer bonds. The first, Zeeman term involves anisotropic g-tensors, and for site 1 is given by

$$\mathbf{g}_1 = \begin{pmatrix} g_x & 0 & -g_s \\ 0 & g_y & 0 \\ -g_s & 0 & g_z \end{pmatrix},$$

while $\mathbf{g}_2$, $\mathbf{g}_3$, and $\mathbf{g}_4$ are obtained from $\mathbf{g}_1$ by symmetry operations of the crystal (figure 1). The sign of the xz-component is opposite for $\mathbf{g}_2$, i.e., g_s represents the staggered component. The diagonal components were determined as $g_x = g_y = 2.05$ and $g_z = 2.28$ from ESR measurements [9]. We estimate $g_s = 0.023$ by assuming that the principal axis of $\mathbf{g}_1$ coincides with that of the electric field gradient at Cu1 nuclei (5.6° from the c-axis [15]), which is nearly perpendicular to the plane containing the four oxygen atoms surrounding one Cu1.

In magnetic fields, the anisotropic Hamiltonian $\mathcal{H}_1$ results in a non-collinear magnetization consisting of four sublattices $\boldsymbol{m}_i = \mathbf{g}_i \cdot \langle \boldsymbol{s}_i \rangle \mu_B$ ($i = 1$–4). We define the uniform and staggered moments on A and B dimers as $\boldsymbol{m}_u^A = (\boldsymbol{m}_1 + \boldsymbol{m}_2)/2$, $\boldsymbol{m}_s^A = (\boldsymbol{m}_1 - \boldsymbol{m}_2)/2$ and $\boldsymbol{m}_u^B = (\boldsymbol{m}_3 + \boldsymbol{m}_4)/2$, $\boldsymbol{m}_s^B = (\boldsymbol{m}_3 - \boldsymbol{m}_4)/2$. The crystal symmetry tells us that an external field $\boldsymbol{H}_{ext} \parallel z$ ($\boldsymbol{H}_{ext} \parallel x$) induces staggered moments $\boldsymbol{m}_s^A \parallel x$ and $\boldsymbol{m}_s^B \parallel y$ ($\boldsymbol{m}_s^A \parallel z$). Such non-collinear moments, unobservable from bulk magnetization measurements, can be accurately detected by ^{11}B NMR. The magnetic hyperfine field acting on a nuclear spin at site i is expressed as $\boldsymbol{H}_i^{hf} = \sum_{j=1}^{4} \mathbf{A}_{ij} \cdot \boldsymbol{m}_j$, where $\mathbf{A}_{ij}$ is the hyperfine coupling tensor between the ith nuclear spin and $\boldsymbol{m}_j$. The projection of $\boldsymbol{H}_i^{hf}$ along $\boldsymbol{H}_{ext}$, denoted as H_i, is obtained from the shift of the NMR frequency.

We first discuss the results for a small field (6.948 T) rotated in the $(\bar{1}10)$- (xz-) plane. The NMR spectra consist of several sets of quadrupole-split lines. Each set was assigned to a particular site based on the known anisotropy of the quadrupole splitting [16]. In figure 2, H_1 is plotted against the angle θ between $\boldsymbol{H}_{ext}$ and the c-axis at several temperatures. By symmetry, $H_2(\theta) = H_1(-\theta)$ and $H_3(\theta) = H_4(\theta)$ (not shown). The θ-dependence can be well fitted by a simple sinusoidal curve (curves in figure 2),

$$\begin{aligned} H_1 + H_2 &= H_u \cos 2\theta + \text{const}, \\ H_1 - H_2 &= H_s \sin 2\theta. \end{aligned} \tag{4}$$

T-dependences of H_u and H_s are plotted in figure 3.

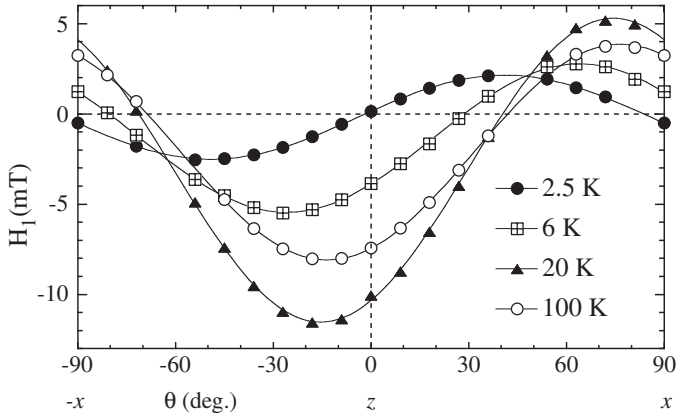

Figure 2. Angular variation of H_1 at different temperatures in the external field of 6.948 T.

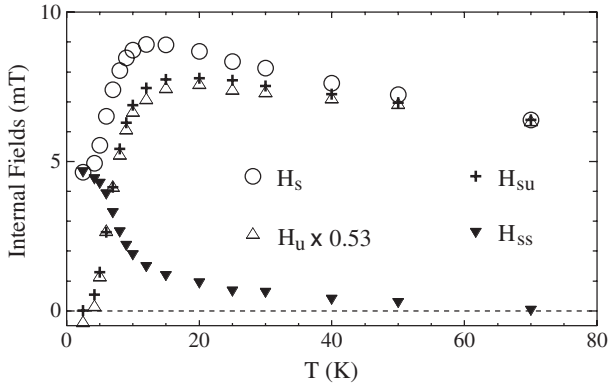

Figure 3. Temperature dependences of H_u, H_s, (4) H_{su}, and H_{ss} (6) at $H_{ext} = 6.948$ T.

The θ-dependence of H_1 is not symmetric around $\theta = 0$, leading to a finite H_s. Both $m_s^{A,B}$ and $m_u^{A,B}$ contribute to H_s through the uniform (diagonal) and the staggered (off-diagonal) parts of the coupling $\mathbf{A}_{ij}$, respectively. If $m_u^{A,B}$ and $m_s^{A,B}$ had the same T-dependence, this should stand for H_s and H_u. This is indeed not the case, since H_s extrapolates to a large finite value at $T = 0$, while H_u almost vanishes similarly to the magnetic susceptibility [4]. This proves that a sizable staggered moment $m_s^{A,B}$ is induced at $T = 0$ at field values $H_{ext} \ll H_c$, while the uniform moment is nearly zero. This can be qualitatively explained by considering $\mathcal{H}_1$ as a perturbation for an isolated dimer [17]. Since $\mathcal{H}_1$ has matrix elements between singlet and triplets on the same dimer, triplets are mixed into the ground state, resulting in finite $m_s^{A,B}$ to first order in perturbation. In contrast, $m_u^{A,B}$ is much smaller than $m_s^{A,B}$, since only higher order terms contribute to $m_u^{A,B}$. Although field-induced staggered moments have been reported in the Haldane chain compound NENP [18, 19], this is the first observation in quasi-2D systems.

For a quantitative analysis, we write

$$\begin{aligned} H_1 - H_2 = {} & 2\,(B_{xz} + C_{xz})\left(m_{uz}^{A}\sin\theta + m_{ux}^{A}\cos\theta\right) \\ & + 2\,(B_{xx} - C_{xx})\,m_{sx}^{A}\sin\theta + 2\,(B_{zz} - C_{zz})\,m_{sz}^{A}\cos\theta \\ & + 4D_{xz}\left(m_{uz}^{B}\sin\theta + m_{ux}^{B}\cos\theta\right) + 4D_{xy}m_{sy}^{B}\sin\theta, \end{aligned} \tag{5}$$

where we have defined $\mathbf{B} = \mathbf{A}_{11}$, $\mathbf{C} = \mathbf{A}_{12}$, and $\mathbf{D} = \mathbf{A}_{13}$ and used symmetry properties to obtain other $\mathbf{A}_{ij}$. The $\sin 2\theta$ dependence of $H_1 - H_2$ in (4) is reproduced if the moments vary as $m^{\mathrm{A}}_{\mathrm{s}x}$, $m^{\mathrm{B}}_{\mathrm{s}y}$, $m^{\mathrm{A,B}}_{\mathrm{u}z} \propto \cos\theta$, and $m^{\mathrm{A}}_{\mathrm{s}z}$, $m^{\mathrm{A,B}}_{\mathrm{u}x} \propto \sin\theta$. This is approximately confirmed by the numerical calculations presented below. We define

$$\sigma_x \equiv m^{\mathrm{A}}_{\mathrm{s}x}(\theta = 0) = m^{\mathrm{B}}_{\mathrm{s}y}(\theta = 0), \qquad \sigma_z \equiv -m^{\mathrm{A}}_{\mathrm{s}z}(\theta = \pi/2),$$
$$M_z \equiv m^{\mathrm{A,B}}_{\mathrm{u}z}(\theta = 0), \qquad M_x^{\mathrm{A(B)}} \equiv m^{\mathrm{A(B)}}_{\mathrm{u}x}(\theta = \pi/2).$$

Combining these relations with (5), we obtain

$$H_{\mathrm{s}} = H_{\mathrm{su}} + H_{\mathrm{ss}} \tag{6}$$
$$H_{\mathrm{su}} = (B_{xz} + C_{xz} + 2D_{xz})\, M_z + (B_{xz} + C_{xz})\, M_x^{\mathrm{A}} + 2D_{xz} M_x^{\mathrm{B}} \tag{7}$$
$$H_{\mathrm{ss}} = \left(B_{xx} - C_{xx} + 2D_{xy}\right)\sigma_x - (B_{zz} - C_{zz})\,\sigma_z. \tag{8}$$

The analysis of the ^{11}B NMR spectrum in the 1/8-plateau phase [20] indicates that all hyperfine couplings except $\mathbf{B}$ are approximately given by the classical dipolar fields that we can calculate. Since the diagonal components of $\mathbf{B}$+$\mathbf{C}$+2$\mathbf{D}$ were determined previously [16], all the coupling parameters in the above equations are known except for B_{xz}. At high temperatures, the staggered moments σ_x, σ_z are much smaller than the uniform moments M_z, $M_x^{\mathrm{A,B}}$, and $M_x^{\mathrm{A}} \approx M_x^{\mathrm{B}}$. Assuming $\sigma_x = \sigma_z = 0$ above $T = 70$ K, which is also supported by preliminary numerical calculations, we determined B_{xz} from the data of H_{s} and the magnetization at 70 K, using (6). The parameters in (7) and (8) are determined as $B_{xz} + C_{xz} + 2D_{xz} = 0.10$, $B_{xz} + C_{xz} = 0.09$, $2D_{xz} = 0.01$, $B_{xx} - C_{xx} + 2D_{xy} = -0.06$, and $B_{zz} - C_{zz} = -0.32$ (T μ_{B}^{-1}). We then obtained H_{su} at other temperatures (figure 3) from the magnetization data. Finally, subtracting this from H_{s}, H_{ss} is determined in the whole temperature range as shown in figure 3. This demonstrates that the staggered magnetization increases very steeply below 10 K and saturates at lower temperatures.

Measurements of H_i were extended to higher fields up to 26 T. The magnetization data in [8] was used to calculate H_{su},[8] which was then subtracted from the data of H_{s} to obtain H_{ss}. In the main panel of figure 4, we plot H_{su} and H_{ss} in the low-temperature limit.

In order to see if these results are explained by anisotropic interactions, we have calculated $\boldsymbol{m}_i$ by exact diagonalization (ED) of the Hamiltonian $\mathcal{H}_0$+$\mathcal{H}_1$+$\mathcal{H}'$ at $T = 0$ and $H_{\mathrm{ext}} = 6.948$ T in the $(\bar{1}10)$-plane for clusters with up to 24 sites for various values of D. Values of other parameters are fixed: $J = 85$ K, $J' = 54$ K [3], $D'/J = -0.02$ [12], and $g_{\mathrm{s}} = 0.023$. By requiring that the calculated value of H_{s} from (6) to (8) agrees with the experimental data at the lowest temperature (2.5 K), we obtained $D/J = 0.034$. Taking into account the uncertainty in g_{s} leads to possible values of D/J between 0.030 (for $g_{\mathrm{s}} = 0.030$) and 0.038 (for $g_{\mathrm{s}} = 0.014$). The choice of D' has little effect on the calculated values of $\boldsymbol{m}_i$.

Using the same parameter values, we have also calculated $\boldsymbol{m}_i$ at higher fields, as shown in the inset of figure 4. The agreement between the calculated results of H_{su} and H_{ss} shown by the lines in the main panel of figure 4 and the experimental data is satisfactory up to about 20 T. Thus we now have a *quantitative* explanation for the development of a uniform magnetization at fields as low as 18 T. Note that the staggered moment is sizable even at low fields ($\sim$0.03 μ_{B}/Cu at 15 T, figure 4 inset), where the uniform moment is negligible. The experimental and theoretical results of H_{ss} deviate at higher fields, probably due to finite-size effects as discussed below.

Let us now discuss the dynamics. The nuclear spin–lattice relaxation rate $(1/T_1)$ was measured for $\boldsymbol{H}_{\mathrm{ext}} \parallel \boldsymbol{c}$ up to 27.5 T. It shows an activated behaviour at low temperatures

[8] We estimated M_x^{A} and M_x^{B} separately by using the magnetization data of $(M_x^{\mathrm{A}} + M_x^{\mathrm{B}})/2$ and assuming the ratio $M_x^{\mathrm{A}}/M_x^{\mathrm{B}} = 2.7$ for the field range 18–26 T as indicated by the ED calculations (figure 4 inset).

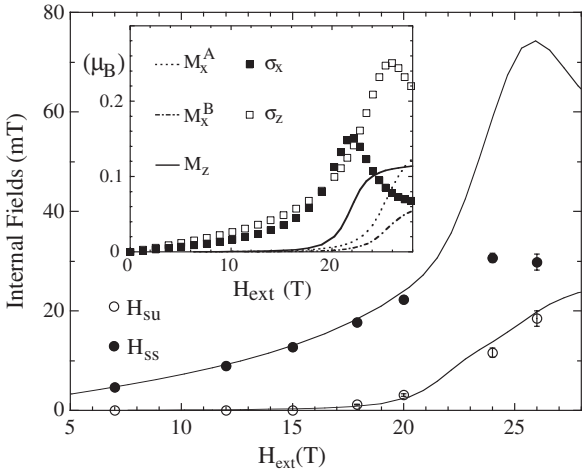

Figure 4. Field dependences of H_{su} and H_{ss} measured at low temperatures, 2.5 K (for $H_{ext} = 7$ and 12 T), 1.5 K (15 and 17.9 T), 0.64 K (20 T), 0.46 K (24 T), and 0.21 K (26 T). The curves are obtained from the ED results of σ_x, σ_z, M_z, and $M_x^{A,B}$ shown in the inset by using (7) and (8).

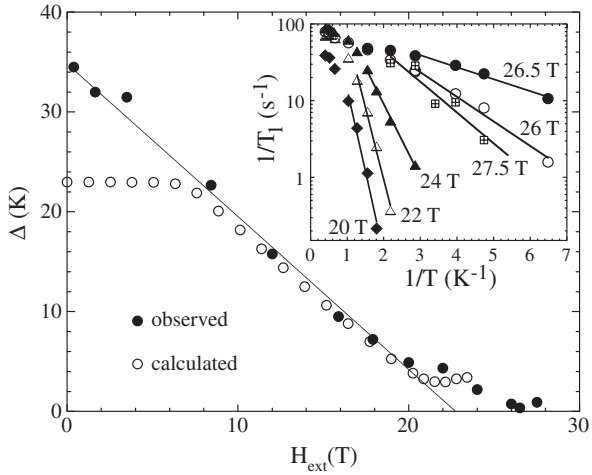

Figure 5. Field dependence of the excitation gap (solid circles in the main panel) determined from the activated behaviour of $1/T_1$ (inset) compared with the results of ED calculation (open circles). The data at 27.5 T, where the NMR spectrum shows many lines in the 1/8-plateau phase, were obtained for the line with the largest (negative) hyperfine field.

(figure 5 inset). The activation gap (Δ) shown in figure 5 follows a linear H-dependence below 20 T, $\Delta = \Delta_0 - g_z\mu_B H$ with $\Delta_0 = 34.8$ K and $g_z = 2.28$ as expected. At higher fields, however, it deviates from this relation and remains finite even above the expected critical field $H_c = \Delta_0/g_z\mu_B = 22.7$ T. The gap reaches a minimum at 26.5 T, which is at the boundary to the 1/8-plateau, and increases again inside the 1/8-plateau (27.5 T). The finite gap above H_c, which naturally explains the absence of Bose condensation, is consistent with earlier reports. For example, the gap was estimated from the specific heat data [11] as $\Delta = 4.6$ (3.2) K at $H_{ext} = 22$ (24) T. The ESR data [10] also show a similar deviation from the linear H-dependence of the lowest triplet energy near H_c.

One expects that the singlet–triplet mixing due to $\mathcal{H}_1$ will prevent the gap from closing, as has been discussed for NENP [21]. We have confirmed this by numerical calculations. The energy of the lowest excited state obtained by ED calculations using the same parameters is plotted in figure 5. The constant value at low fields is due to the singlet bound state of two triplets having lower energy than one triplet [22]. However, they do not contribute to the nuclear relaxation. Near 22 T, the results clearly indicate level repulsion due to mixing, reproducing the experimental behaviour. Let us note one subtle point. The interdimer DM interaction $\mathcal{H}'$ splits the one-triplet excitations into two branches [12]. Only one of them is mixed with the singlet by $\mathcal{H}_1$ and this branch must have a lower energy for the level repulsion to occur. This determines the sign of D' to be negative. Note that the sign of D' was not known before.

Finally, the theory is not applicable when the field is too close to the $1/8$-plateau. The cluster size of our calculation is not large enough to take proper account of interaction between triplets, which should become important near the $1/8$-plateau.

In conclusion, we have shown that a large staggered magnetization is induced by the magnetic field in the presence of the intradimer DM interaction and staggered g-tensor, whose magnitudes are obtained as $0.03 \leqslant D/J \leqslant 0.038$ for $0.014 \leqslant g_{\mathrm{s}} \leqslant 0.03$. The singlet–triplet mixing and level repulsion caused by these interactions account for the finite uniform magnetization below H_{c} and the persistence of the excitation gap above H_{c}. They thus turn the quantum phase transition at H_{c} into a crossover. This is the first example of such field-induced phenomena in quasi-2D spin systems. Our determination of the magnitudes and sign of the DM interactions should set the stage for further investigation of other remarkable properties of $SrCu_2(BO_3)_2$. In particular, the signature of a phase transition in the specific heat observed above the $1/8$-plateau by Tsujii *et al* [11] calls for a precise understanding of the interplay between the DM interaction and other bosonic interaction such as bound state formation [22] and correlated hopping [23].

We thank M Oshikawa, K Ueda, and T Ziman for stimulating discussions. This work is supported by Grants-in-Aid for Scientific Research from the MEXT Japan and by the Swiss National Fund.

References

[1] Rice T M 2002 *Science* **298** 760
[2] Tanaka H *et al* 2001 *J. Phys. Soc. Japan* **70** 939
[3] For a review, see Miyahara S and Ueda K 2003 *J. Phys.: Condens. Matter* **15** R327
[4] Kageyama H *et al* 1999 *Phys. Rev. Lett.* **82** 3168
[5] Onizuka K *et al* 2000 *J. Phys. Soc. Japan* **69** 1016
[6] Kodama K *et al* 2002 *Science* **298** 395
[7] Miyahara S and Ueda K 1999 *Phys. Rev. Lett.* **82** 3701
Miyahara S and Ueda K 2000 *Phys. Rev.* B **61** 3417
[8] Kageyama H *et al* 2001 *J. Alloys Compounds* **317/318** 177
[9] Nojiri H *et al* 1999 *J. Phys. Soc. Japan* **68** 2906
[10] Nojiri H *et al* 2003 *J. Phys. Soc. Japan* **72** 3243
[11] Tsujii H *et al* 2003 *Preprint* cond-mat/0301509
[12] Cépas O *et al* 2001 *Phys. Rev. Lett.* **87** 167205
[13] Kageyama H *et al* 1999 *J. Cryst. Growth* **206** 65
[14] Smith R W and Keszler D A 1991 *J. Solid State Chem.* **93** 430
[15] Kodama K *et al*, unpublished
[16] Kodama K *et al* 2002 *J. Phys.: Condens. Matter* **14** L319
[17] Miyahara S *et al* 2004 *J. Phys.: Condens. Matter* **16** S911
[18] Chiba M *et al* 1991 *Phys. Rev.* B **44** 2838

[19] Fujiwara N *et al* 1993 *Phys. Rev.* B **47** 11860
[20] Kodama K *et al*, unpublished
[21] Mitra P P and Halperin B I 1994 *Phys. Rev. Lett.* **72** 912
[22] Knetter C *et al* 2000 *Phys. Rev. Lett.* **85** 3958
Fukumoto Y 2000 *J. Phys. Soc. Japan* **69** 2755
Totsuka K, Miyahara S and Ueda K 2001 *Phys. Rev. Lett.* **86** 520
[23] Momoi T and Totsuka K 2000 *Phys. Rev.* B **61** 3231
Momoi T and Totsuka K 2000 *Phys. Rev.* B **62** 15067